Available online at www.sciencedirect.com

ScienceDirect

Journal of Magnesium and Alloys 6 (2018) 15–22

www.elsevier.com/locate/jma

Full Length Article

Improvement in the corrosion protection and bactericidal properties of AZ91D magnesium alloy coated with a microstructured polypyrrole film

A.D. Forero López[a], I.L. Lehr[a], L.I. Brugnoni[b], S.B. Saidman[a,*]

[a] *Instituto de Ingeniería Electroquímica y Corrosión (INIEC), Departamento de Ingeniería Química, Universidad Nacional del Sur, Av. Alem 1253, 8000 Bahía Blanca, Argentina*

[b] *Instituto de Investigaciones Biológicas y Biomédicas del Sur (INBIOSUR), Departamento de Biología, Bioquímica y Farmacia, Universidad Nacional del Sur, San Juan 670, 8000 Bahía Blanca, Argentina*

Received 3 March 2017; received in revised form 18 December 2017; accepted 25 December 2017
Available online 17 March 2018

Abstract

In this work hollow rectangular microtubes of polypyrrole (PPy) films were potentiostatically electrodeposited on magnesium alloy AZ91D in salicylate solution. The substrate was previously anodized under potentiostatic conditions in a molybdate solution in order to improve the adherence of polymer. Finally the duplex film was modified by the incorporation of silver species. The obtained coatings were characterized by scanning electron microscopy (SEM), X-ray diffraction (XRD) and X-ray photoelectron spectroscopies (XPS) and the antimicrobial activity against the bacteria *Escherichia coli* was evaluated. The corrosion protection properties of the coatings were examined in Ringer solution by monitoring the open circuit potential, polarization techniques and electrochemical spectroscopy (EIS). The duplex coating presents an improved anticorrosive performance with respect to the PPy film. The best results concerning corrosion protection and antibacterial activity were obtained for the silver-modified composite coating.

Keywords: Polypyrrole; Duplex coating; AZ91D alloy; Corrosion resistance; Antibacterial properties.

1. Introduction

The biodegradability of magnesium-based materials constitutes an advantage for developing temporary therapeutic devices [1–3]. However, the rapid corrosion of these materials alloys under physiological conditions has delayed their introduction for therapeutic applications to date [2].

Significant efforts have been made to modify the surface of Mg alloys in order to improve their corrosion resistance. Among surface modification methods, electrodeposited conducting polymers are promising candidates as protective coatings. Polypyrrole is one of the most studied conducting polymers due to its relatively easy preparation, high chemical stability and relatively low potential for electropolymerization. In particular, Mg alloys covered with PPy constitutes a biodegradable and biocompatible platform for controlled release of therapeutic drugs [2,4].

Several studies on the corrosion inhibition of Mg alloy AZ91D involving PPy were reported. A PPy layer was prepared in aqueous sodium tartrate solution by introducing a zinc electroplating layer between the alloy and the PPy layer [5]. It has been also demonstrated that sodium salicylate doped PPy layer shows good corrosion protection property in Na_2SO_4 solutions [6,7]. It was found that a salicylate solution was the best electrolyte used for the electrosynthesis of PPy onto other Mg alloys [8,9]. In this medium dissolution of the alloys is significantly reduced.

Our previous studies also demonstrated that the salicylate solution is an electrolytic medium that allows the electrosynthesis of PPy with a particular structure. Hollow rectangular microtubes of PPy were synthesized onto 316L stainless steel and onto Nitinol in neutral and alkaline solutions of salicylate

* Corresponding author.
E-mail addresses: ssaidman@criba.edu.ar, dflamini@uns.edu.ar (S.B. Saidman).

https://doi.org/10.1016/j.jma.2017.12.005

(Sa) [10,11]. It was proposed that microtubes were templated by salicylic acid (HSa) crystals which crystallize on the electrode surface as a result of the decrease in pH that accompanies the electrodeposition. The formation of rectangular tubes requires a high salicylate concentration in a stagnant solution.

The incorporation of bactericidal substances into polymer matrices, such as polypyrrole, is of interest in the design of new biomaterials. It is well known that silver ions or metallic silver as well as silver nanoparticles are antibacterial agent and possess low toxicity to human cells [12]. The electrosynthesis of a PPy coating doped with Sa was an effective substrate for Ag species immobilization and the modified electrodes had an excellent biocide effect [11,13]. In this paper, we show the first attempts to synthesize a PPy coating constituted by hollow rectangular microtubes onto an Mg alloy. The corrosion resistance properties as well as the capacity of the films to incorporate silver species were evaluated.

2. Materials and methods

The working electrodes were prepared from rods of *die-cast* AZ91D magnesium alloy (composition: 8.978% Al, 0.6172% Zn, 0.2373% Mn, 0.2987% Si, 0.1189% Cu, 0.00256% Ni, 0.0176% Fe, 0.00164% Ca, 0.01154% Zr, balance Mg**).** The rods were embedded in a Teflon holder with an exposed area of 0.070 cm^2. Before each experiment, the exposed surfaces were polished to a 1000 grit finish using SiC, then degreased with acetone and washed with triply distilled water. Following this pretreatment, the electrode was immediately transferred to the electrochemical cell. All the potentials were measured against a saturated Ag/AgCl and a platinum sheet was used as a counter electrode. The cell was a 20 cm^3 Metrohm measuring cell.

The electrodes were treated in an electrolyte solution containing 0.50 M sodium salicylate (NaSa) and 0.50 M pyrrole (Py). Solutions were purified with a saturated atmosphere of nitrogen gas at 25 °C. Pyrrole (Py, Sigma-Aldrich) was freshly distilled under reduced pressure before use. The pH of the solution was adjusted by addition of NaOH. All chemicals were reagent grade and solutions were made in twice distilled water.

Electrochemical measurements were done using a potentiostat–galvanostat Autolab/PGSTAT 128 N and VoltaLab40 Potentiostat PGZ301. A dual stage ISI DS 130 SEM and an EDAX 9600 quantitative energy dispersive X-ray analyzer were used to examine the electrode surface. X-ray diffraction analysis was carried out using a Rigaku X-ray diffractometer (model Dmax III-C) with Cu Kα radiation and a graphite monochromator. X-ray photoelectron spectroscopy (XPS) has been measured in a Specs setup operating. The XPS analysis chamber is equipped with a dual anode (Al/Mg) X-ray source and a 150 mm hemispherical electron energy analyzer (PHOIBOS). The analyzer operates in fixed analyzer transmission (FAT) mode with pass energy of 30 eV. The energies of all spectra were referenced to the C 1s peak at 285.0 eV. All the XPS spectra were deconvoluted using the Casa XPS software with a Gaussian–Lorentzian mix function**.**

Film adhesion was tested measuring the force necessary to peel-off the film using a Scotch® MagicTM double coated Tape 810 (3 M) and a Mecmesin basic force gauge (BFG 50 N). Electrical conductivity was measured by two-probe method using a homemade device.

The corrosion behavior was evaluated in Ringer solution at 37 °C by the variation of the open circuit potential (OCP) as a function of time, by a potentiodynamic method and by electrochemical impedance spectroscopy (EIS). The electrodes were allowed to equilibrate at the fixed voltage before the ac measurements. The composition of Ringer solution is (per 1 L) 8.60 g NaCl, 0.30 g KCl and 0.32 g $CaCl_2$•$2H_2O$.

The Tafel tests were carried out by polarizing from cathodic to anodic potentials with respect to the open circuit potential at 0.001 V s^{-1} in Ringer solution. Estimation of corrosion parameters was realized by the Tafel extrapolation method. The extrapolation of anodic and/or cathodic lines for charge transfer controlled reactions gives the corrosion current density (i_{corr}) at the corrosion potential (E_{corr}). All experiments were conducted after the steady-state E_{corr} was attained. Measurements were repeated four times for each coating investigated to ensure reproducible and significant data.

The antibacterial activity against a reference strain of *E. coli* ATCC 25922 was evaluated by a modified Kirby–Bauer technique [14]. The method was previously standardized by adjusting the microbial inoculation rate and the volume of the agar medium layer. A freezing culture of *E. coli* ATCC 25922 (stored at −70 °C in Tripticase Soy Broth (TSB) (BK 046HA, Biokar Diagnostics, Beauvais, France) supplemented with 20% (v/v) glycerol (Biopack, Argentina) was used. A loop of frozen cells was cultured in TSB during 24 h at 37 °C. Upon appropriate dilution with sterilized phosphate buffer saline solution, a suspension of about 10^7 cells mL^{-1} was prepared. One milliliter of this suspension was mixed with 25 ml of Tripticase Soy Agar (BK, Biokar Diagnostics, Beauvais, France) melted and cooled at 43 °C, and then, placed on a Petri dish. The coated electrodes were pressed onto bacteria-overlaid agar and were incubated at 37 °C for 24 h. Then they were removed from the agar and placed in a fresh one. The data were expressed as growth inhibitory zone diameter (mm) for three replicates [15]. Control tests employing unmodified PPy-coated electrodes were also performed.

3. Results and discussion

3.1. Polypyrrole coating

Hollow rectangular-sectioned microtubes of polypyrrole were deposited under potentiostatic conditions [10,16]. An active dissolution of the AZ91D alloy at the electropolymerization potential is expected from thermodynamic considerations. First, potentiostatic polarization curves in monomer-free solution are presented (Fig. 1). The figure shows the curves obtained at 1.15 V in 0.5 M NaSa (curve a) and in 0.50 M $NaNO_3$ (curve b) solutions. Alloy dissolution is observed in NO_3^- at this high potential while passivation is achieved in Sa solution.

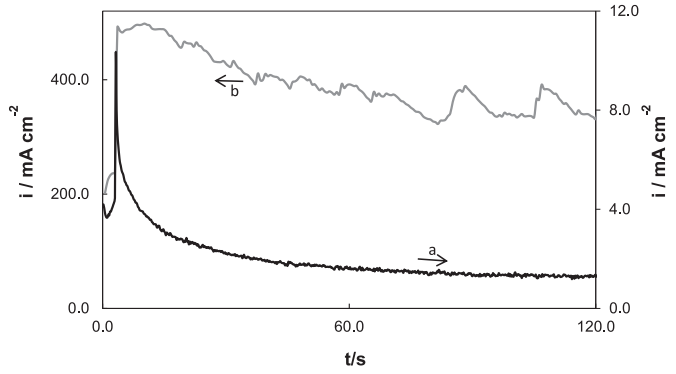

Fig. 1. Potentiostatic transients obtained at 1.15 V for 30 min in: (a) 0.50 M NaSa, pH 7 and (b) 0.50 M $NaNO_3$, pH 7 solutions.

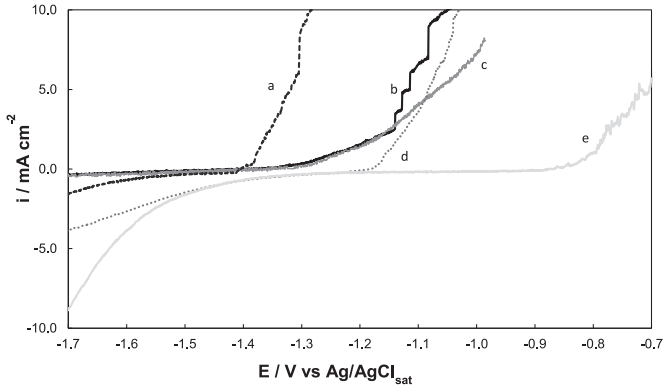

Fig. 3. Polarization behavior in Ringer solution at 37 °C for: (a) uncoated AZ91D alloy; (b) PPy-pH 7, (c) PPy-pH 12, (d) Mo-coat/PPy and (e) Mo-coat/PPy-Ag. The scan rate was 0.001 V s^{-1}.

Electropolymerization is very difficult when a strong dissolution of the substrate initiates at potentials more negative than that corresponding to the oxidation of the monomer. That is why no electropolymerization occurs in NO_3^- solution. In contrast, the electrode is passivated in Sa solution enabling PPy electrodeposition The electrosynthesis was performed at 1.15 V during 600 s in a solution containing 0.50 M salicylate and 0.50 M Py. A black coating was deposited at the end of the experiment. The SEM image of the sample shows rectangular sectioned microtubes, being the majority of them oriented parallel to the electrode surface (Fig. 2). The typical granular morphology of PPy is also observed.

Close to two H^+ ions per Py monomer polymerized are released during the polymerization process [17]. This local pH decrease at the interface produces the protonation of salicylate anion and then salicylic acid crystallizes due to its low solubility [10]. Further polymerization occurs at the external surface of the HSa crystals. If Mg dissolution occurs at this high positive potential needed for polymerization, Mg^{2+} hydrolysis should contribute to a lowering of the local pH [18]. Thus, in the case of Mg alloy as a substrate the local pH variation at the interface should not be an impediment to the microtubes formation.

The anodic polarizations of uncoated alloy and PPy-covered electrode in Ringer solutions are presented in Fig. 3. The curve corresponding to the bare alloy shows that hydrogen evolution reaction occurs until active dissolution initiates at −1.43 V (Fig. 3, curve a). Anodic polarization corresponding to the polymer formed in solution containing 0.50 M NaSa, pH 7 (PPy-pH 7) (Fig. 3, curve b) exhibits the onset for the current increase shifted 100 mV in the positive direction. Thus, the curves indicate that the coating has little effect on the corrosion behavior of the alloy. This is related

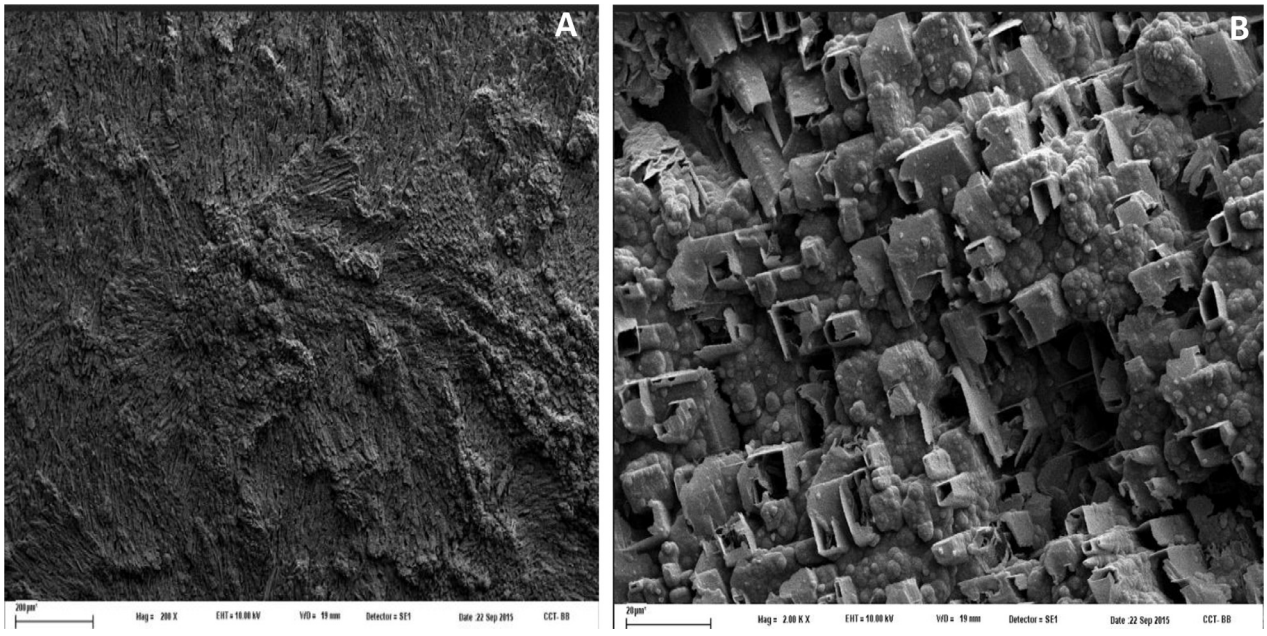

Fig. 2. SEM micrographs of a PPy coating formed on AZ91D alloy obtained at different magnifications: (a) 200x and (b) 2000x. The film was electrosynthesized at 1.15 V during 600 s in 0.50 M NaSa + 0.50 M Py, pH 7 solution.

Table 1
Adherence force obtained for the different coatings after peel-off testing.

Coating	Adherence force (N)
PPy-pH 7	9.73
Mo-coat	24.95
Mo-coat/PPy	24.90
Mo-coat/PPy-Ag	22.05

with the fact that the PPy film was not well adhered to the substrate. Moreover the opened structure of the hollow rectangular microtubes coating allows the corrosive medium to penetrate toward the substrate.

PPy structures with a rectangular cross-section can also be generated by electropolymerization in alkaline solutions of salicylate [16]. Because there is a competition between salicylate oxidation and PPy deposition, electrosynthesis is favored when the potential is raised to 1.3 V. The use of alkaline solutions promotes the formation of a more protective magnesium oxide/hydroxide film which should be beneficial for electropolymerization [18]. But the polymer formed at pH 12 (PPy-pH 12) was not a protective film either, as can be observed in Fig. 3, curve c. It was considered that a thick layer of $Mg(OH)_2$ or MgO formed on Mg alloys during anodic polarization prevents the formation of an adhesive PPy coating [19].

3.2. Polypyrrole coating deposited on anodized AZ91D alloy

It was demonstrated that a low-voltage anodization in molybdate solution was effective in lowering the corrosión rate of AZ91D when exposed to Ringer solution [20]. The best results were obtained when the Mg alloy was anodically polarized at 1.0 V (Ag/AgCl) during 2700 s in MoO_4^{2-} solution. In order to slow down the corrosion rate of the alloy in chloride medium the anodized film was formed on the electrode surface prior to the electropolymerization process. For simplicity this anodized film will be named Mo-coat. When the first film was formed in MoO_4^{2-} solution during 2700 s, as we done in our previous work [20], no polymer was obtained. To find the optimum thickness of the inner layer, films were formed at different times prior to PPy electrosynthesis in Sa solution. For an anodization time of 300 s the polymer electrosynthesized in Sa solution only presents patches of deposits with rectangular morphology due to the high thickness of the first layer. A PPy film covering the whole electrode was obtained when the inner layer was formed during 20 s. The PPy coating obtained on the Mo-coat is characterized by the presence of microtubes of different size coexisting with the typical globular morphology (Fig. 4). It will be named Mo-coat/PPy.

The adherence forces measured for the alloy covered by PPy and by the Mo-coat/PPy coating were 9.73 N and 24.90 N, respectively (Table 1). It can be concluded that there is not good adhesion between the PPy coating and the substrate and that the Mo-coat layer formed before

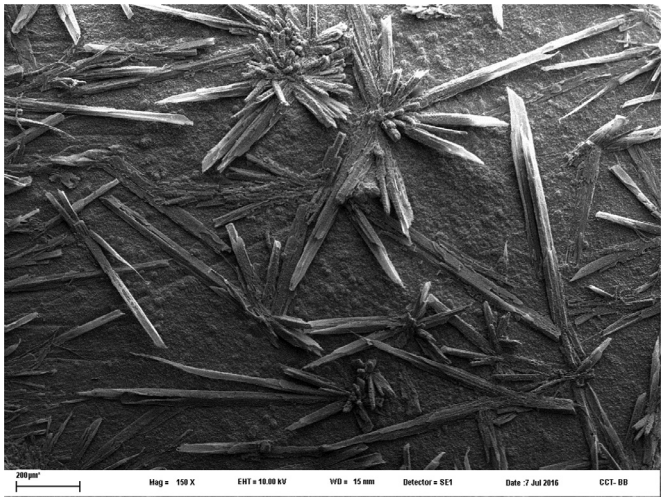

Fig. 4. SEM micrograph of the Mo-coat/PPy coating.

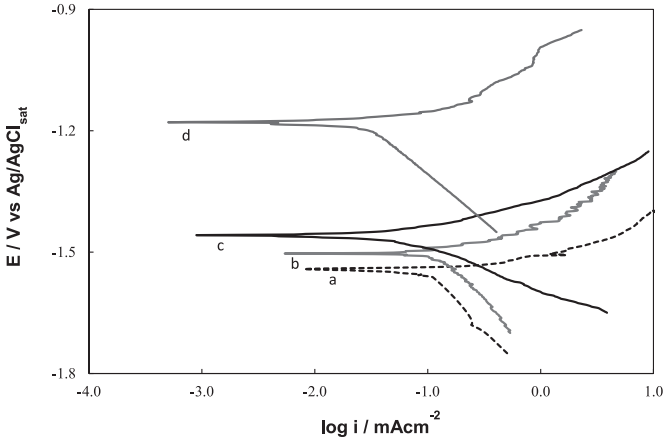

Fig. 5. Tafel curves obtained in Ringer solution at 37 °C for: (a) uncoated AZ91D, (b) PPy film, (c) Mo-coat/PPy and (d) Mo-coat/PPy-Ag.

electropolymerization promotes the synthesis of a more adherent PPy film.

In order to evaluate the corrosion resistance of the modified electrode, anodic polarization was conducted in Ringer solution (Fig. 3, curve d). As can be seen, in this case the current density increases at more positive potentials in comparison to that for the PPy-covered alloy, indicating dissolution retardation.

More information concerning corrosion resistance of the covered electrodes can be obtained through Tafel polarization curves in Ringer solution. The polarization behavior of the sample covered with the duplex layer is compared with those corresponding to the single PPy layer and the bare alloy (Fig. 5). It should be mentioned that the redox phenomena of the polymer occur simultaneously with the corrosion reaction. As was reported in various publications the estimation of the corrosion current density for a metal coated with a conducting polymer by linear polarization is difficult because some of the measured current arises from the redox activity of the polymer [21–23]. In spite of this, according to the

Table 2
Corrosion parameters calculated from Tafel polarization plots for uncoated AZ91D; PPy film; Mo-coat/PPy and Mo-coat/PPy-Ag. The mean values and their standard deviation are presented.

	E_{corr} (V)	i_{corr} (mA cm^{-2})	β_a (V)	β_c (V)
AZ91D	–1.501 ± 0.050	0.1050 ± 0.0050	0.045	–0.293
PPy-pH 7	–1.456 ± 0.030	0.112 ± 0.0050	0.080	–0.235
Mo-coat/PPy	–1.415 ± 0.020	0.060 ± 0.0050	0.084	–0.113
Mo-coat/PPy-Ag	–1.130 ± 0.020	0.027 ± 0.0050	0.058	–0.223

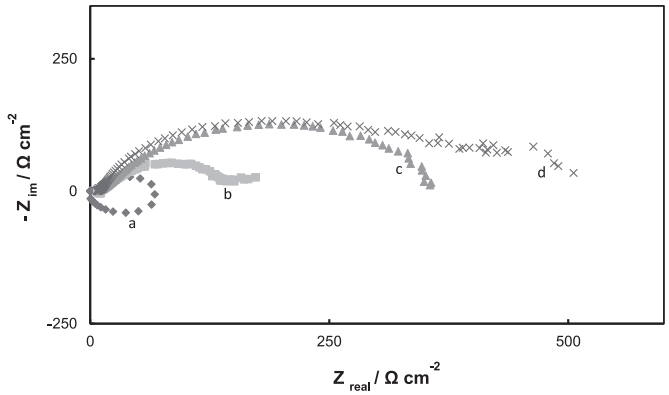

Fig. 6. Nyquist plots of the impedance spectra obtained at the open circuit potential in Ringer solution at 37 °C after 5 min of immersion for: (a) uncoated AZ91D alloy, (b) PPy film, (c) Mo-coat/PPy and (d) Mo-coat/PPy-Ag.

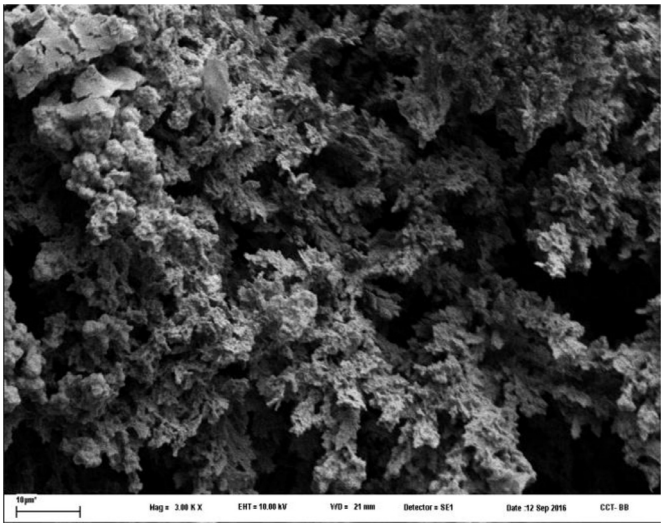

Fig. 7. SEM micrograph of Mo-coat/PPy-Ag coating.

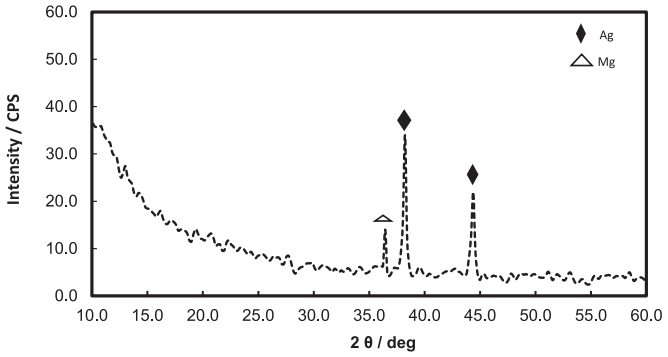

Fig. 8. XRD spectrum for Mo-coat/PPy-Ag.

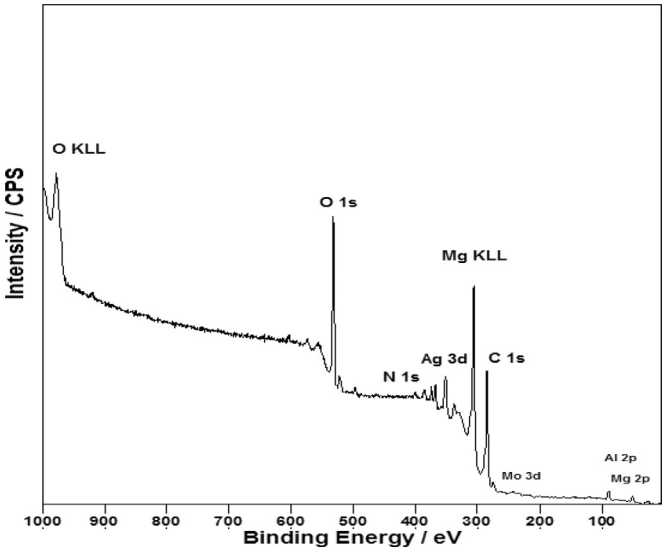

Fig. 9. XPS survey spectrum of Mo-coat/PPy-Ag coating formed on AZ91D alloy.

results shown in Fig. 5 as well as in Table 2, an increase in the corrosion potential (E_{corr}) is accompanied by a smaller corrosion current density (i_{corr}) in the case of Mo-coat/PPy electrode.

EIS measurements confirm the Tafel polarization curves results. The impedance spectra of the samples after immersing in Ringer solution are presented in Fig. 6. The frequency used for the impedance measurements was changed from 100 kHz to 10 mHz, and the signal amplitude was 10 mV. In the case of the bare electrode the EIS response presents two capacitive loops and one inductive loop. The inductive loop was attributed to the relaxation processes of adsorbed species such as $Mg(OH)^+$or $Mg(OH)_2$ on the electrode surface. This process is not observed for Mo-coating/PPy which indicates there is no interaction between the metal surface and the corrosive solution, proving again that corrosion is inhibited for the treated sample. Semicircles diameter corresponds to the polarization resistance. The Mo-coat/PPy presents a higher polarization resistance and then a higher corrosion resistance than the bare alloy.

It is considered that a conducting polymer in its conductive state acts as an efficient oxidizer to maintain the metal in the passive state [24]. Moreover the Sa-doped PPy may release the anion dopant upon reduction, which is a corrosion inhibitor for the substrate. In the case of the duplex coating, the first layer formed by anodization in MoO_4^{2-} solution improves the adherence of the PPy film as well as the corrosion resistance of the Mg alloy.

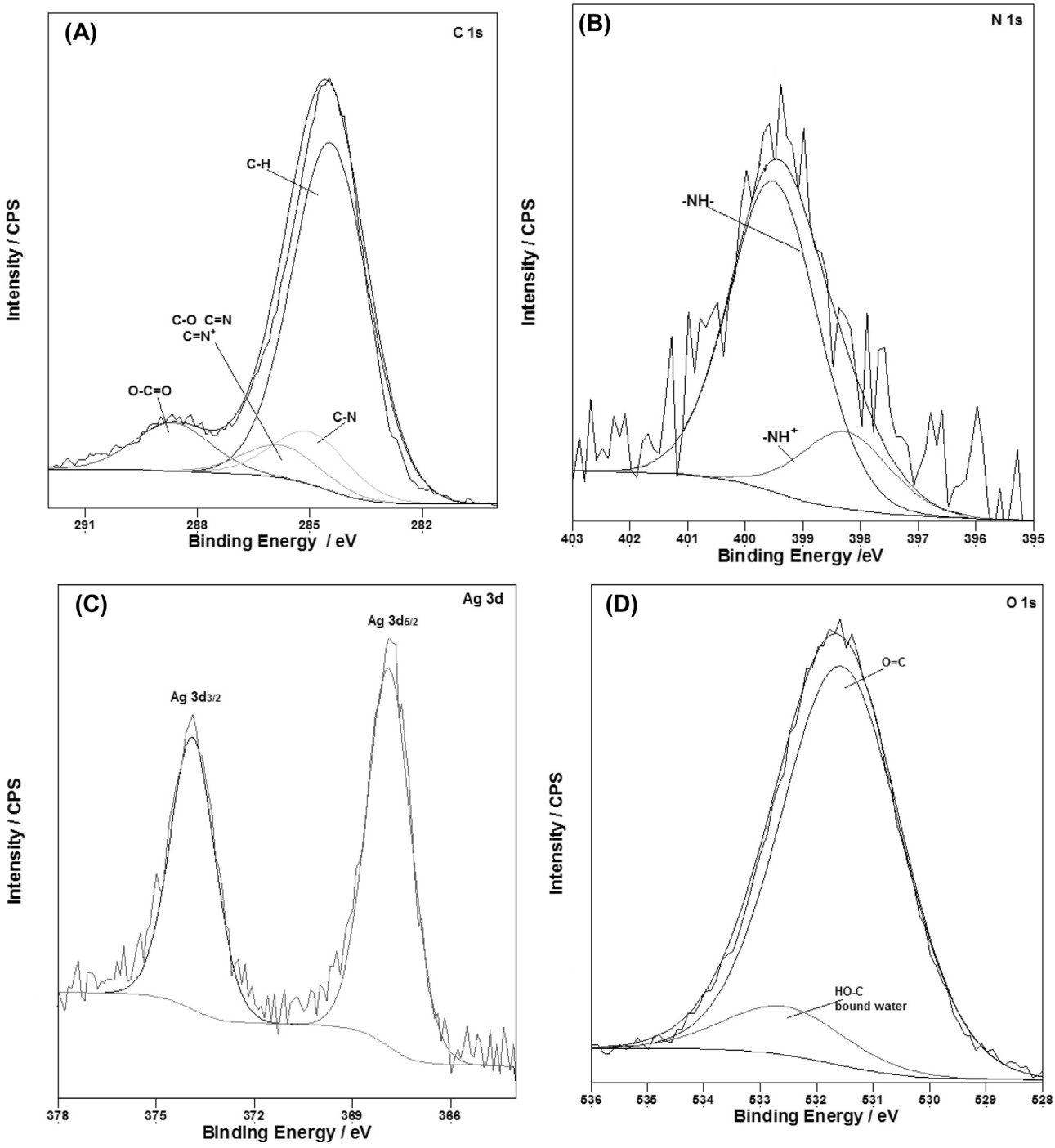

Fig. 10. XPS intensities of: (A) C 1s; (B) N 1s; (C) Ag 3d and (D) O 1s.

3.3. Silver deposition

The Mo-coat/PPy-covered electrodes were left in an $AgNO_3$ solution during 2 h under open circuit conditions. SEM examination after immersion shows that silver dendrites were obtained in a large quantity on the PPy coating (Fig. 7). The modified fill will be named Mo-coat/PPy-Ag. XRD analysis of the coating confirms the presence of silver. Two intense diffraction peaks detected at 2θ values of 38.14° and 44.34° correspond to the Bragg reflections to the planes of Ag (111) and (200) (Fig. 8).

The elemental and chemical composition of the Mo-coat/PPy-Ag coating was determined by XPS. According to the XPS survey spectra (Fig. 9), it can be seen the peaks corresponding to Mg 2p, O 1s, Mo 3d, N 1s, C 1s and Ag 3d. A more detailed XPS analysis of the specific electron binding energies of C, N, O and Ag elements is presented (Fig. 10). As shown in Fig. 10A, the C 1s spectrum can be fitted into

Table 3
Concentration of magnesium species released in Ringer solution after 5 h of immersion of uncoated and coated AZ91D alloy.

Sample	Mg (mg/L)
AZ91D	3.95
PPy-pH 7	3.30
Mo-coat/PPy	2.10
Mo-coat/PPy-Ag	1.23

four peaks with the following assignments: 284.4 eV, β carbons of the pyrrolic chains and aromatic carbons of Sa/HSa (salicylate and salicylic acid) and adventitious C; 285.1 eV, α carbons of the pyrrole chains; 286.4 eV the C–O of the alcoholic functions of Sa/HSa, C=N of the pyrrole rings and the bipolarons ($–C=N^+$) and 288.6 eV, the carboxylate of Sa/HSa [10,25–27].

The N 1s peak (from the polypyrrole ring), centered at 399.2 eV is displayed in Fig. 10B and was deconvoluted into two peak components at 399. 5 and 401.2 eV associated to the –NH– and $–N^+–$ species [28–30]. As can be seen from the Fig. 10C the characteristic Ag $3d_{3/2}$ (373.5 eV) and Ag $3d_{5/2}$ (367.7 eV) peaks are observed, indicating that Ag is present in the coating as elemental silver [27,31,32]. The spectrum of O 1s is presented in Fig. 10D. The peak located at 531.6 eV is assigned to O=C and the peak at 533.6 eV corresponding to HO–C and bound water [33]. The peaks of Mg 2p ($E_b \approx$ 52 eV) and Mo 3d ($E_b \approx$ 234 eV) are not shown because they are very weak and noisy. This result is probably associated to the high thickness of PPy film modified with Ag.

The anion Sa plays a key role in the immobilization of silver species into the coating [13]. It was proposed that Ag^+ ions are concentrated in the film as a result of the interaction between Sa with Ag^+. Metallic silver was deposited as a result of a redox reaction between no oxidized segments of the polymer and Ag^+ ions.

A higher corrosion protection of the alloy was attained after Ag deposition on the Mo-coat/PPy coating. Active dissolution of the alloy starts at more positive potentials as can be seen in Fig. 3. Moreover the Ag-modified film exhibits a higher corrosion potential and a lower corrosion current density than the others coatings (Fig. 5 and Table 2). The i_{corr} is reduced by about one order of magnitude. This improvement is in part associated with a filling of pores in the PPy coating.

In order to confirm the improvement in the corrosion performance of the AZ91D magnesium alloy the quantity of Mg released under OCP conditions in Ringer solution during 5 h of immersion was analyzed for the different samples (Table 3). The lowest quantity released corresponds to the substrate covered with Mo-coat/PPy modified with Ag corroborating its better performance. Moreover, the obtained results confirm that the PPy films provided poor corrosion resistance.

The conductivity of the coatings was evaluated using two-probe conductivity measurements. The results showed that the conductivity value of Mo-coat/PPy film modified with silver (1.2×10^{-3} S cm^{-1}) is one order of magnitude higher than the unmodified bilayer (1.4×10^{-4} S cm^{-1}). It has been reported that the structure and electrical conductivity of conducting polymers strongly affect their anticorrosive properties [34–36]. Moreover, several studies demonstrated that an open structure provided less corrosion protection and that these films showed low conductivity values. The obtained results demonstrated that the higher conductivity corresponds to Mo-coat/PPy coating modified with Ag which also shows a superior anticorrosive performance.

As was mentioned earlier the microstructured PPy film was not well adhered so it was easily detached from the alloy surface. On the contrary, the Ag-modified as well as the unmodified duplex coating could be removed only by mechanical polishing. The necessary force to peel-off the last two coatings had the same order of magnitude (Table 1).

One of the most important advantages of dendritic structures is their large effective surface area. Thus, the Ag-modified PPy can constitute an effective antimicrobial biomaterial. In order to check this, we investigated the antibacterial activity of immobilized silver against the Gram negative bacteria *E. coli* ATCC 25922 by determining the width of the inhibition zone around the coated surfaces.

It is well known that when an antibacterial material is in contact with bacterial strain, a clear area around the material is formed, and it is referred to as zone of inhibition [37]. Antibacterial activity of Mo-coat/PPy film was detected against *E. coli* ATCC 25922 consisting of an inhibition zone of approximately 5 mm surrounding the sample. However, when the coating is modified with silver, this inhibition area is notoriously increased (13 mm). Moreover, the results indicate that the inhibitory efficiency of coated electrodes is practically independent of the immersion time in the $AgNO_3$ solution during the coating preparation. The penetration of the released Ag^+ ions and colloid silver particles through the bacteria cell wall explains the antibacterial properties.

4. Conclusions

A microstructured polypyrrole coating was formed potentiostatically on the biodegradable AZ91D magnesium alloy. Because of the opened structure of the hollow rectangular microtubes and poor adhesion of the deposited film the corrosion protection was low.

Improvement in adhesion may be attained by forming a duplex coating consisting of a first film obtained by anodization of AZ91D alloy in molybdate solution and a second layer of polypyrrole electrosynthesized in salicylate media. The inner film promotes the electrodeposition of an adherent and stable polymer.

The duplex coating is able to retard the corrosion of the substrate under OCP conditions in Ringer solution. This result is explained considering the protective properties of the inner film, the ability of the polymer to maintain the metal in the passive state and the inhibitor characteristics of salicylate.

The duplex film was modified by the incorporation of silver particles under open circuit potential conditions. This coating presents better corrosion protection properties because Ag particles seal porosity of the film and increases its

conductivity. The Ag-modified bilayer exhibits also good antibacterial activity against *E. coli*. Thus, the coating is a promising material for future biomedical applications with antibacterial properties.

Acknowledgment

CONICET (PIP-112-201101-00055), ANPCYT (PICT-2012- 0141) and Universidad Nacional del Sur (PGI 24/M127), Bahía Blanca, Argentina are acknowledged for financial support.

References

[1] S. Agarwal, J. Curtin, B. Duffy, S. Jaiswal, Mater. Sci. Eng. C 68 (2016) 948–963.
[2] Q. Chen, G.A. Thouas, Mater. Sci. Eng. R 87 (2015) 1–57.
[3] G. Wu, J.M. Ibrahim, P.K. Chu, Surf. Coat. Technol. 233 (2013) 2–12.
[4] S.E. Moulton, M.D. Imisides, R.L. Shepherd, G.G. Wallace, J. Mater. Chem. 18 (2008) 3608–3613.
[5] N. Sheng, Y. Lei, A. Hyonoo, M. Ueda, T. Ohtsuka, Prog. Org. Coat. 77 (2014) 1724–1734.
[6] M.C. Turhan, M. Weiser, H. Jha, S. Virtanen, Electrochim. Acta 56 (2011) 5347–5354.
[7] M.C. Turhan, M. Weiser, M.S. Killian, B. Leitner, S. Virtanen, Synth. Met. 161 (2011) 360–364.
[8] Z. Grubač, I.Š. Rončević, M.M. Huković, Corros. Sci. 102 (2016) 310–316.
[9] M. Hatami, M. Saremi, R. Naderi, Prog. Nat. Sci. Mater. Int. 25 (2015) 478–485.
[10] M.B. González, O.V. Quinzani, M.E. Vela, A.A. Rubert, G. Benítez, S.B. Saidman, Synth. Met. 162 (2012) 1133–1139.
[11] M. Saugo, D.O. Flamini, L.I. Brugnoni, S.B. Saidman, Mater. Sci. Eng. C 56 (2015) 95–103.
[12] F. Paladini, M. Pollini, A. Sannino, L. Ambrosio, Biomacromolecules 16 (2015) 1873–1885.
[13] M.B. González, L.I. Brugnoni, M.E. Vela, S.B. Saidman, Electrochim. Acta 102 (2013) 66–71.
[14] V. Maquet, D. Martin, B. Malgrange, R. Franzen, J. Schoenen, G. Moonen, R. Jérôme, J. Biomed. Mater. Res. 52 (2000) 639–651.
[15] P.T.S. Kumar, S. Abhilash, K. Manzoor, S.V. Nair, H. Tamura, R. Jayakumar, Carbohydr. Polym. 80 (2010) 761–767.
[16] M.B. González, S.B. Saidman, Electrochem. Commun. 13 (2011) 513–516.
[17] S. Sadki, P. Schottland, N. Brodie, G. Sabouraud, Chem. Soc. Rev. 29 (2000) 283–293.
[18] L. Rossrucker, A. Samaniego, J.P. Grote, A.M. Mingers, C.A. Laska, N. Birbilis, G.S. Frankel, K.J.J. Mayrhofer, J. Electrochem. Soc. 162 (2015) 333–339.
[19] N. Sheng, T. Ohtsuka, Prog. Org. Coat 75 (2012) 59–64.
[20] A.D. Forero Lopez, I.L Lehr, S.B. Saidman, J. Alloys Compd. 702 (2017) 338–345.
[21] M.A. Arenas, L. Gónzalez Bajos, J.J. de Damborenea, P. Ocón, Prog. Org. Coat. 62 (2008) 79–86.
[22] D.O. Flamini, S.B. Saidman, Corros. Sci. 52 (2010) 229–234.
[23] V. Annibaldi, A.D. Rooney, C.B. Breslin, Corros. Sci. 59 (2012) 179–185.
[24] S. Biallozor, A. Kupniewska, Synth. Met. 155 (2005) 443–449.
[25] K.F. Babu, P. Dhandapani, S. Maruthamuthu, M.A. Kulandainathan, Carbohydr. Polym. 90 (2012) 1557–1563.
[26] C. Wan, J. Li, Carbohydr. Polym. 146 (2016) 362–367.
[27] L. Yuan, C. Wan, X. Ye, F. Wu, Electrochim. Acta 213 (2016) 115–123.
[28] S.W. Huang, K.G. Neoh, E.T. Kang, H.S. Han, K.L. Tan, J. Mater. Chem. (8) (1998) 1743–1748.
[29] X. Yang, L. Li, S. Shang, G. Pan, X. Yu, G. Yan, Mater. Lett. 64 (2010) 1918–1920.
[30] L. Viau, J.Y. Hihn, S. Lakard, V. Moutarlier, V. Flaud, B. Lakard, Electrochim. Acta 137 (2014) 298–310.
[31] B. Horváth, J. Kawakita, T. Chikyow, Appl. Surf. Sci. 384 (2016) 492–496.
[32] C. Wang, S. Zanna, I. Frateur, B. Despax, P. Raynaud, M. Mercier-Bonin, P. Marcus, Surf. Coat. Technol. 307 (2016) 1–8.
[33] L. Ruangchuay, J. Schwank, A. Sirivat, Appl. Surf. Sci. 199 (2002) 128–137.
[34] C.K. Tan, D.J. Blackwood, Corros. Sci. 45 (2003) 545–551.
[35] A. Olad, M. Barati, H. Shirmohammadi, Prog. Org. Coat. 72 (2011) 599–604.
[36] I.L. Lehr, S.B. Saidman, Prog. Org. Coat. 76 (2013) 1586–1593.
[37] C.L. Gallant-Behm, H.Q. Yin, S.J. Liu, J.P. Heggers, R.E. Langford, M.E. Olson, D.A. Hart, R.E. Burrell, Wound Repair Regener 13 (2005) 412–421.